Proceedings World Geothermal Congress 2015
Melbourne, Australia, 19-25 April 2015

Analysis of Stress Heterogeneities in Fractured Crystalline Reservoirs

David Sahara, Martin Schoenball, Thomas Kohl, Birgit Mueller

Karlsruhe Institute of Technology, Adenauerring 20b, 76131 Karlsruhe, Germany

david.sahara@student.kit.edu

Keywords: stress field, borehole breakout, fracture network, geo-reservoir

ABSTRACT

The present day state of stress has a key influence on fluid flow through fractured geo-reservoirs. Wellbore breakouts are commonly used as the principal indicator of stress direction. However, variation of breakout orientation with depth, especially in the vicinity of fracture zones, is frequently observed. This study describes a systematic analysis of breakout occurrence, variation of breakout orientation and its modeling. Numerical modeling which takes into account the elastic property changes as a result of fracturing and fracture filling is developed to better quantify the very local scale breakout orientation heterogeneity observed in this study. Two different mechanisms for the breakout rotation are proposed. Anomalies of breakout orientation in the vicinity of fracture zones reflect the large-scale stress heterogeneity which might be caused by the previous slip acting on the fault plane. The local breakout orientation anomalies around minor fractures might be the effect of the material heterogeneities around borehole due the intersection between the borehole with the fracture. The results of this study provide a better understanding of stress-induced borehole elongations in fractured rocks. Borehole breakout heterogeneities do not seem to be related to the principal stress heterogeneity only, but also to the effect of mechanical heterogeneities like weak zones with different elastic moduli, rock strength and fracture patterns. Consequently, care has to be taken when inferring the principal stress orientation from borehole breakout data observed in fractured rock.

1. INTRODUCTION

The key component of a comprehensive geomechanical model is knowledge of the current state of stress. Wellbore failure occurs because the stress concentrated around the circumference of a well exceeds the strength of the rock (Moos et al., 2003). A fault will slip when the ratio of shear to effective normal stress acting on the fault plane exceeds its frictional strength (Scholz, 2002). Depletion cause changes in the stress state of the reservoir that can be beneficial or harmful to production in a number of ways (Zoback, 2007). Determination of the state of stress at depth in a georeservoir is a problem that can be addressed with data that are routinely obtained when wells are drilled, i.e. hydraulic fracturing, borehole breakouts, drilling induce tensile fracture (DITF) and many others.

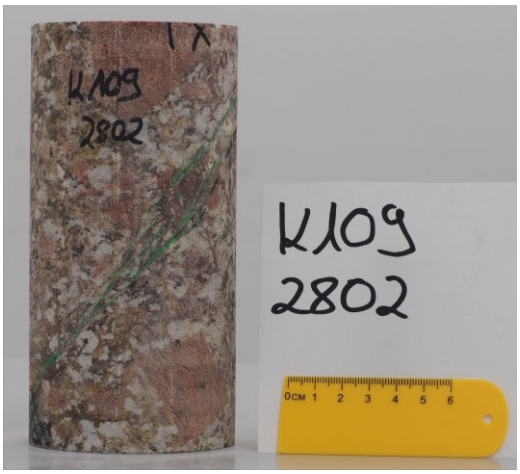

Figure 1: One example of fracture observed in drill-core from Soultz-sous-Forêts. Interpreted microcracks are drawn in green lines.

Borehole breakouts are cross-sectional elongations in the minimum horizontal stress direction, which are caused by localized failure around a borehole due to stress concentrations (Bell and Gough, 1979; Zoback et al., 1985). Breakouts are one of the direct indicators of the contemporary tectonic stress field. However, breakout orientations can vary and differ from the mean minimum horizontal stress orientation.

The source of these deviations remain unclear. Paillet and Kim (1987) suggested that slip on active faults penetrated by boreholes was the source of breakout anomalies. Barton and Zoback (1994), Shamir (1990) and Shamir and Zoback (1992) computed the local stress perturbation in the vicinity of fractures, which is required to distort the breakout orientation based on slip on the fault plane. In their studies, near complete stress drop on the fracture plane (around 26 MPa at 5400 m depth) is required to match the observed breakout orientation anomalies by this model. In other publications, it is also suggested that such heterogeneity might also be related to minor fracture densities (Sikaneta and Evans, 2012) or to fluid pressure (Chang and Haimson, 2006).

In this paper we consider the changes in mechanical properties affecting the breakout orientation, in particular the Young's modulus and the Poisson's ratio, induced by the high microcrack density of the fault zone. Fault zones have a high microcrack density near the fault core. This microcrack density decreases exponentially with distance from the fault core (Vermilye and Scholz, 1998). One example of increasing microcrack density in the fracture core observed in a drill core in Soultz-sous-Forêts is shown in Figure 1. Changes of rock mechanical parameters due to changing crack density could lead to local heterogeneous zones around the fault core (Heap and Faulkner, 2008). Faulkner et al. (2006) showed that crack density influences the elastic properties of rock and, hence, the stress state of surrounding faults. Furthermore, they found that the mean stress as well as the magnitude of the highest principal stress decrease and the least principal stress increase as the fault core is approached, resulting in overall decrease in the differential stress. Thus, the breakout orientation anomalies might also be attributed to varying crack density.

Sahara et al. (submitted) analyzed breakouts patterns in a 5 km deep well in the enhanced geothermal system in Soultz-sous-Forêts (France). He clearly identified breakout orientation rotations in the vicinity of both major fracture zones and minor fractures. He suggested that the breakout anomalies around minor fractures might be the effect of the material heterogeneities around borehole due the intersection between the borehole with the fracture. Following the work from Sahara et al. (submitted), numerical modeling of the stress field distribution around a borehole in a heterogeneous model is developed. The results of this modeling is expected to better characterize how the natural fracture network is affecting the stress distribution around borehole and eventually altering the breakout shape and orientation.

2. BREAKOUT HETEROGENEITY OBSERVATION

The principal horizontal stress orientation deviations are observed at various scales. Regional scale of stress heterogeneities have stress pattern wavelengths of tens of kilometer around the Alps (Heidbach et al., 2007; Müller et al., 1997). Local scale variations can be a few hundred meters in the vicinity of major fracture zones (Barton and Zoback, 1994; Valley and Evans, 2007), and even more local scale variations can occur in the circumference of a minor fracture (Sahara et al., submitted). These second or even third-order stress patterns indicate that localized sources of stress, such as gravitational potential energy of the elevated Alpine orogeny, lateral density and strength contrasts, stress perturbation following a slip on an active fault or even more localized sources can locally overrule the far-field stress contribution.

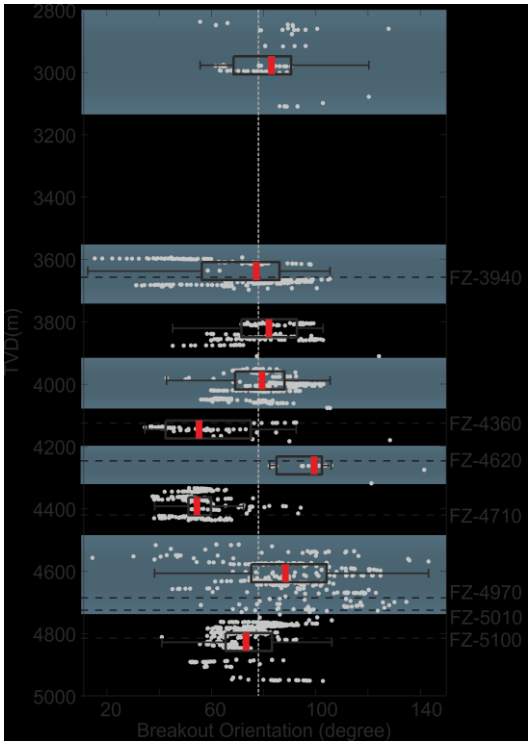

Figure 2: Profile of breakout orientations in the GPK4 well. Box plots are used to summarize the distribution of depth intervals. The lower and upper fences, the 1st and 3rd quartiles (rectangle) as well as the median value are plotted. The depths of the intersected major fractures are indicated by dashed lines (modified after [*Sahara et al.*, submitted]

Following is one typical example of how the breakout orientations vary with depth in a deep well in Soultz-sous-Forêts, France. In-situ stress orientation and magnitude of the Soultz-sous-Forêts geothermal field were inferred from borehole log and hydraulic methods in previous studies. Cornet et al. (2007) reviewed various reports and analyses on hydraulic tests, borehole images and induced seismicity. In general, the mean maximum horizontal stress orientation values fall within the range of N164°E to 185°E.

Figure 2 shows the one-sided breakout plot of the breakout orientation with depth in one of the deep wells in Soultz-sous-Forêts geothermal field, France. The breakouts reveal that the average orientation of the minimum horizontal stress is N78° ± 17°E. The azimuthal deviations represented in each box plot can be considered as including measurement errors, local heterogeneities and variations of the stress orientation.

In the vicinity of the fracture zone FZ-4360, most of the observed breakout orientations are rotated from ASh in the counterclockwise direction. The median is found to be deviated by 13°. However, breakouts were absent in the vicinity of the FZ-4360 fracture core. A similar breakout absent zone was observed in several other fields, e.g. [7, 36]. The role of the FZ-4360 fracture zone seems to prevent breakout formation in its vicinity. This suggests that the magnitude of the differential stresses is reduced in the immediate vicinity of FZ-4360. Possible mechanisms are plasticity or creep (Sibson, 1977).

Only a few breakouts are observed in the vicinity of FZ-4620. All those breakouts are oriented toward the clockwise direction from ASh (Figure 7). FZ-4710 is found about 80 m below FZ-4620. This fracture zone is a Hercynian fracture intersecting the GPK4 well with the lowest inclination (Hurd and Zoback, 2012; Ziegler, 1994). Around the fracture zone, breakouts have the highest orientation rotation at the fault core. Breakout orientation trends were dominated by negative shifts. It is suggested that the fault initiated the breakout, starting from the borehole elongation towards the azimuth of the fault dip (clockwise 46° deviation) and gradually returns to ASh with increasing distance from the fault core. The two distinct breakout patterns in the vicinity of FZ-4360 and FZ-4710 fracture zones suggest the role of fracture zones in breakout heterogeneity, either in preventing breakout occurrence or rotating their orientation.

Sahara et al. (submitted) showed that some minor fractures also perturbed breakout orientation. It is interesting since the dimensions of natural fractures are too small to induce local stress perturbations required to alter the breakouts orientation (Barton and Zoback, 1994). It was concluded that it is the effect of the material heterogeneities around borehole due the intersection of the borehole and the fracture. In this case, the breakout rotation, relative to the mean Shmin direction, is strongly influenced by the fracture orientation. In some depth intervals, a direct relationship between fracture and breakout orientations was found.

3. LOCAL BREAKOUT PERTURBATION MODELING

We intend to model the effect of the material heterogeneities on the stress distribution around borehole and eventually calculate the yield criterion to model the breakout perturbation. The effect of fractures on the mechanical properties of rock was analyzed in many studies. In-situ laboratory measurements on Soultz-sous-Forêts granite (Valley, 2007) revealed the effect of fractures on rock mechanical parameters. Young's modulus of intact Soultz-sous-Forêts granite was determined to be around 54 GPa, but only 39 GPa for significantly fractured granite. Furthermore, the uniaxial compressive strength is also found to decrease with increasing fracture density (Alm et al., 1985).

Table 1: List of elastic properties used in this modeling

Parameter	Intact rock	Weak zone
Young's modulus	**40 GPa**	**24 GPa**
Poisson's ratio	**0.36**	**0.42**
Applied far field stress		
SHmax	**55 MPa**	
Shmin	**110 MPa**	
Friction Coefficient	**0.9**	**0.8**

2.3 Stress distribution around borehole

Following the procedure developed by Airy (1862) and described by Timoshenko and Goodier (1970), a particular form of the field equation for general isotropic and plane strain could be derived as,

$$e\left(\frac{\partial^2\sigma_{xx}}{\partial_x^2}+\frac{\partial^2\sigma_{xx}}{\partial_y^2}+\frac{\partial^2\sigma_{yy}}{\partial_x^2}+\frac{\partial^2\sigma_{yy}}{\partial_y^2}\right)+e'\left(\frac{\partial\sigma_{xx}}{\partial_x}+\frac{\partial\sigma_{yy}}{\partial_x}+\frac{\partial\sigma_{xx}}{\partial_y}+\frac{\partial\sigma_{yy}}{\partial_y}\right)=0 \quad (1)$$

where

$$e=\frac{1-\vartheta^2}{E}$$

E and ϑ are Young's modulus and Poisson's ratio of the rock, respectively. For a homogeneous material *e'* is zero, hence Equation 1 could be simplified to

$$e\left(\frac{\partial^2\sigma_{xx}}{\partial_x^2}+\frac{\partial^2\sigma_{xx}}{\partial_y^2}+\frac{\partial^2\sigma_{yy}}{\partial_x^2}+\frac{\partial^2\sigma_{yy}}{\partial_y^2}\right)=0 \quad (2)$$

or

$$\left(\frac{\partial^2}{\partial_x^2}+\frac{\partial^2}{\partial_y^2}\right)(\sigma_{xx}+\sigma_{yy})=0$$

The commonly used Kirsch analytical solution was derived from Equation 2 that satisfies a specific boundary condition suitable for the borehole problem. It is difficult to analytically solve Equation 1 for the borehole problem, however it is clear that for the heterogeneous material the stress distribution depend on the elastic properties of the material (Young's modulus and Poisson's ratio).

Numerical modeling is used to compute the stress distribution around the wellbore in heterogeneous material. We use the commercial finite element software Abaqus (Simulia). Boundary conditions are chosen after Ewy (1993), i.e. the outer nodes are fixed, inner nodes of the wellbore wall are free. At the beginning of the simulation the nodes at the wellbore wall are fixed to simulate the undisturbed rock. Drilling of the well is simulated by instantaneous release of this boundary condition. We calculate the stress evolution from the initial undisturbed rock to the final state in 20 steps. We could also simulate the effect of the weight of the drilling mud, which is used to stabilize the wellbore wall, by additionally applying a radial pressure to the wellbore wall. The parameters used in this simulation are listed in the Table 1.

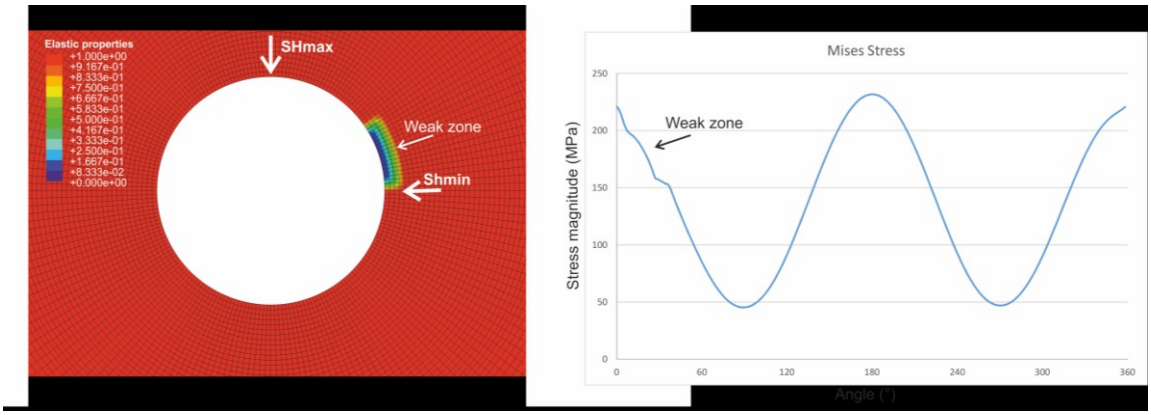

Figure 3: The mesh used in the numerical modeling (left). Narrow and thin weak zone were modeled the intersection with the fracture. Weak zones has lower elastic properties compare to the surrounding material. Stress distribution at the borehole wall (right). The occurrence of the weak zone promote a lower stress region.

Figure 3 (left) shows the mesh used in this simulation. The weak zone was modeled by a zone with lower elastic properties. An elastic properties reduction of 40% from the intact rock was applied in the center of the weak zone. Gradual changes in elastic properties were applied at the boundary of the weak zone to make the numeric calculation stable. In this model, the weak zone is set close to the Shmin direction to highlight the stress changes due to the weak zone. The distribution of stresses distribution around the borehole is concentrated in the Shmin direction, hence the highest stress perturbation due to weak zone is expected to happen in this direction.

We can see in the Figure 3 (right) a small weak zone, comparable to the size of the damage zone due to fractures, alters the stress distribution around boreholes. The stress magnitude at the weak zone is lower than that in the homogeneous material. The stress perturbation seems to be concentrated in the weak zone. This result is in agreement with the Equation 1 which shows that, for heterogeneous isotropic elastic material, the stress distribution around borehole depends on the elastic properties of the material. We have tried several models with different elastic properties of the weak zone but with the same percentage of the material reduction relative to the intact rock. Models which have higher elastic properties at the weak zone also have higher intact rock properties. Interestingly, the stress distribution at the borehole wall are the same. It seems that the stress distribution outside a hollow inclusion depends mainly on the elastic properties difference of the material, rather than its absolute value.

The same procedure was applied to some model with different elastic properties contrast between the weak zone and the intact rock. The results are plotted in Figure 4. Here we plotted the stress reduction, relative to the homogeneous case, as function of the elastic properties reduction of the weak zones. Three stress invariant, Mises stress (q), pressure stress (p), and third invariant of the deviatoric stress (r) are plotted in this figure, as we will use those stresses in calculating the yield criterion in the next subchapter. Mises stress (q) and pressure stress (p) are calculated from first and second principal invariants of the Cauchy stress as:

$$p = \frac{1}{3} I_1 \qquad (3)$$

$$q = \sqrt{3 J_2}$$

Where I_1 and J_2 and J_3 are the first invariant of Cauchy stresses and the second invariant of the deviatoric stresses, respectively.

2.3 Yield criterion and breakout formation

The Mohr-Coulomb failure or strength criterion has widely been used for geotechnical applications. Indeed, a large number of the routine design calculations in the geotechnical area are still performed using the Mohr-Coulomb criterion. The Mohr-Coulomb criterion assumes that failure is controlled by the maximum shear stress and that this failure stress depends on the normal stress. This can be represented by plotting Mohr's circle for states of stress at failure in terms of the maximum and minimum principal stresses. The Mohr-Coulomb failure line is the straight line that touches these Mohr's circles. Thus the Mohr-Coulomb criterion can be written as,

$$\tau = c - \sigma \tan\varphi \qquad (4)$$

where τ is the shear stress, σ is the normal stress (negative in compression), c is the cohesion of the material, and φ is the material angle of friction.

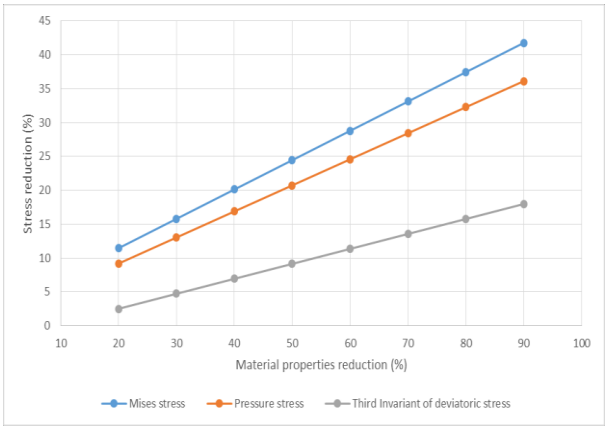

Figure 4: Graphic of the stress concentration perturbation due to the occurrence of a weak zone as a function of the weak zone material properties. Three invariant stresses are showed, Misses stress (blue), Pressure stress (orange) and Third invariant of the deviatoric stress (grey)

The constitutive model described here is an extension of the classical Mohr-Coulomb failure criterion. It is an elastoplastic model that uses a yield function of the Mohr-Coulomb form. Yield function is chosen because its easiness to extend the formulation for elastoplastic problem which includes isotropic hardening/softening to the model. The elastoplastic model will be very useful in modeling breakout beyond its yield strength. However, in this study we limited our model to the elastic mode.

The Mohr-Coulomb criterion written above in terms of the maximum and minimum principal stresses can be written for general states of stress in terms of three stress invariants. These invariants are the Mises stress (q), pressure stress (p), and the third invariant of the deviatoric stress (r). The Mohr-Coulomb yield surface is then written as

$$F = R_{mc}q - ptan\varphi - c = 0 \quad (5)$$

where R_{mc} is the Mohr-Coulomb deviatoric stress measure defined as

$$R_{mc}(\theta,\varphi) = \frac{1}{\sqrt{3}cos\varphi}\sin\left(\theta + \frac{\pi}{3}\right) + \frac{1}{3}cos\left(\theta + \frac{\pi}{3}\right)tan\varphi \quad (6)$$

and θ is the deviatoric polar angle defined as

$$\cos(3\theta) = \left(\frac{r}{q}\right)^3 \quad (7)$$

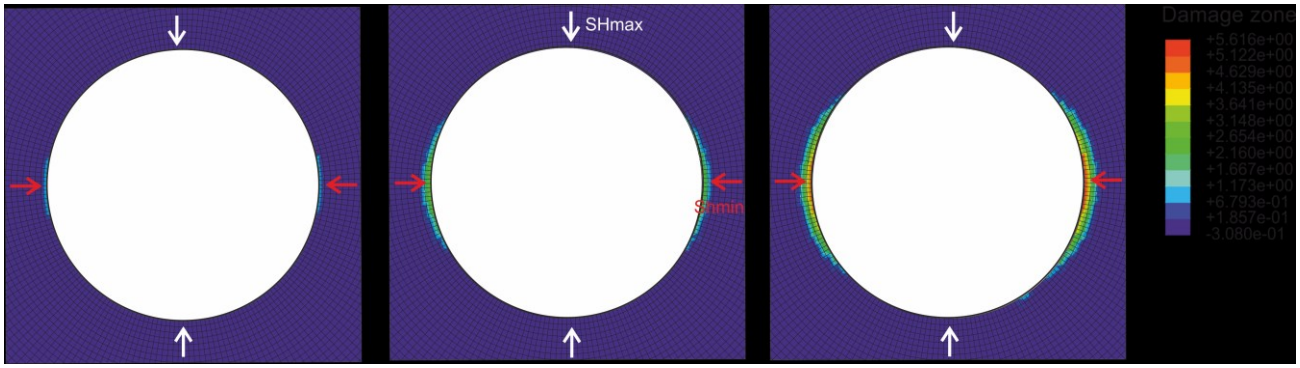

Figure 5: Damage zone evolution due to the stress concentration around borehole. The damage state of each element is described by the damage variable D, which takes the value D = 0 for undamaged and increase with further failure. Hence, the higher number of D shows the higher damage state.

We tested our modeling procedure in calculating the shear and normal stresses and modelled the damaged zone in the homogeneous model. The damaged zone is defined as the zone in which acting stresses have reached the yield surface. The step failure model is incorporated into Abaqus using a subroutine. Here the damage state of the model is read and updated according to the current stress state at each time step. Figure 5 shows the damage evolution around the borehole. Damage starts at the 14th step of the simulation at the direction of minimum horizontal stress, where the stresses are concentrated, and continue growing wider and deeper. As a result, two symmetric damage zones in the opposite direction are formed. The shapes of these damaged zones are consistent with a standard breakout as proposed by Zoback et al., (1985).

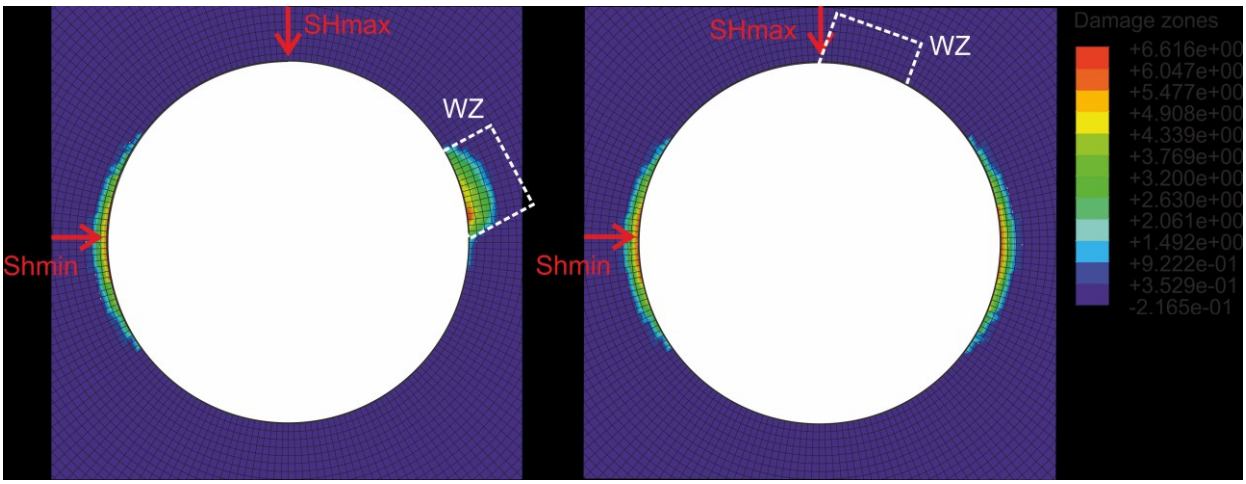

Figure 6: The final damage zone modeled in the heterogeneous material with the weak zone is located in the vicinity of Shmin direction (left) and SHmax direction (right).

The same procedure was then applied for the heterogeneous material. The same model as Figure 3 was used. The weak zone is only modeled in one side of the borehole as a single fracture typically only created a single weak zone. Here, we run the simulation in two cases. First the weak zone is set in the vicinity of the minimum horizontal stress direction, while in the second run it was moved close to the maximum horizontal stress direction. This was done by switching the direction of the minimum and the maximum horizontal stresses. The purpose is to model how the stress perturbation around these weak zones alter the calculated damage zone.

Increased crack density leads to degradation of the elastic moduli, thus reducing the capability of rock to support stress (Heap et al., 2010; Kemeny and Cook, 1986). Hence the friction coefficient value was also lowered at the weak zone (Table 1). In the first model, we can see that the failure was initiated in the weak zone and then followed by the failure in the minimum horizontal stress direction (Figure 6 left). The damage zones then develop according to this initial failure. As a result, an asymmetric damage zone pair is formed. The orientation of the modeled breakout is perturbed by the occurrence of the weak zone and rotated from the Shmin direction. In this case we have to be careful since the breakout orientations do not show the true direction of the minimum horizontal stress, instead it was affected by the weak zone.

It was not the case for the second run. Here a symmetric breakout shape parallel to the direction of the minimum horizontal stress esulted (Figure 6 right). The strength degradation at the weak zone was not significant enough to facilitate the breakout to be developed in the weak zone. In the direction of Shmax, the stresses are less concentrated so it is difficult to reach the yield criterion here prior to the Shmin direction. A huge reduction of material strength is required to facilitate the damage to be developed in the Shmax direction.

4. DISCUSSIONS

Breakout orientation heterogeneities are well observed in the vicinity of both major and minor fractures. The dimensions of natural fractures are, however, too small to induce local stress perturbations required to alter the breakouts orientation (Barton and Zoback, 1994). Hence, we attribute the observed small wavelength breakout rotation in the vicinity of a natural fracture to the material heterogeneity due to the occurrence of weak zones in the vicinity of fractures.

Based on the results of a simple heterogeneous model of stress perturbations around the borehole, a hypothesis of the breakout orientation rotation in the vicinity of a fracture could be developed as follows. If a fracture has an associated fractures damage zone, the stresses are expected to be perturbed and rotated depending on the change in elastic properties of the damaged material. As the fracture core bears the most damage, the stress perturbation is assumed to be concentrated in that zone and to decrease with distance to the core. Breakouts will then develop according to this local stress perturbation. In such a case, a gradual breakout orientation rotation centered at the fault core is expected to result. This gradual rotation trend starting from the fault core is observed well in the vicinity of GPK4-FZ4620 (Figure 2).

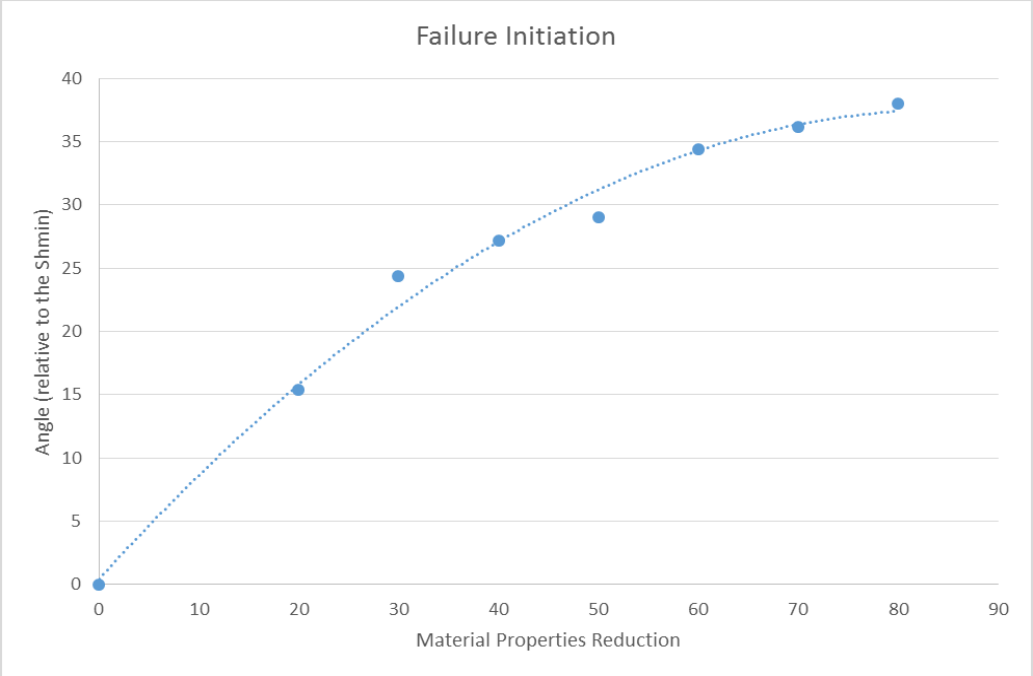

Figure 7: Graphic of the perturbing weak zone position as a function of the elastic properties contrast. Material properties reduction is in percent relative to the intact rock elastic properties.

However, the critical question is under what condition is the breakout orientation perturbed? The possibility could range widely from the material properties of the intersection zone, the stress heterogeneities that might occur, and the technical problems during drilling (i.e. mud pressure, borehole inclination, etc). In this study, we neglect the drilling variable and limited the problem to the breakout orientation perturbation in the vicinity of the minor fracture. Hence we could use a uniform far field stress acting on a heterogeneous inclusion model. Under this assumption, the development of the breakout is only as a function of the stress field acting at the borehole wall and the rock strength to support the stress. The intersection of the borehole wall and the fracture could affect both factors, i.e. reducing the elastic properties hence alter the stress concentration and reducing the capability of rock to support stress.

Though we only modeled in the elastic mode, and not beyond this yield failure, breakouts will grow depending on this initial failure. Furthermore, after the yield strength of the material has been reached, stress will concentrate in this damage zone and the damage will concentrate in this zone. Hence the simulation developed in this study could be used as a basis to model the breakout heterogeneity. The results of the simulation in the previous chapter show that, though the different weak zone position (with the same elastic properties contrast) show the same magnitude of the stress perturbation, the resulting damage zones are different. Hence we could conclude that the breakout perturbations depend on the weak zone elastic properties contrast relative to the intact rock and its position relative to the minimum horizontal stress.

A set of models with different position and elastic properties of the weak zone have been run under several different differential stress magnitudes. Changes in the elastic properties of the rock were assumed to be linear with the rock strength changes of the rock. From the simulation results, a graphic of the position of the perturbing weak zone relative to the minimum horizontal stress direction as a function of the weak zone elastic contrast with the intact rock could be created (Figure 7). The area below the line show the perturbing weak zones position for each weak zone with a specific elastic properties contrast. The higher degradation of the elastic moduli of the weak zones, the higher possibility to alter the breakout formation at a greater angle from the Shmin direction.

Interestingly this graphic is constant for different stress field. Undoubtedly the different differential stress will generate different magnitude of stress distribution around borehole, i.e. Kirsch's solution. Higher differential stress will result in higher stress concentration and vice versa. However here we only discuss the stress distribution slightly before the first failure. In this case, the difference is that at a higher differential stress the yield stress is easier to be reached, i.e. earlier step in this simulation. And it makes the final breakout shape wider and deeper for the higher differential stress, but will not changing the role of the weak zone to alter the breakout shape.

5. CONCLUSIONS

Analyzing breakout heterogeneities and their correlation with fracture occurrence at great depth is a challenging task, in particular because of lacking information on in-situ material properties of fractured rock. We proposed two different mechanisms for the breakout rotation in the vicinity of fracture zones and natural fractures. For breakouts around fracture zones, examples of systematic sinusoidal perturbations to breakout orientation, initiation and inhibition of breakout formation were presented. Therefore we concluded that anomalies of breakout orientation in the vicinity of fracture zones reflect the large-scale stress heterogeneity caused by the fracture zones.

Since it was found that natural fractures are too small to perturb the stress field even locally, the observed perturbations of breakout orientation cannot be explained by a perturbation of the stress field. A numerical model of stress distribution around borehole that incorporates the material heterogeneities could explain the observed breakout heterogeneities in this field. It was shown that for heterogeneous isotropic elastic material, the stress distribution around borehole is dependent on the elastic properties of the material. It improves the analytical formulation of the stress distributions which developed under homogeneous material assumption, i.e. Kirsch solution. A graphic showing the perturbing weak zone position as a function of the elastic properties contrast is presented. Furthermore, the results presented in this study might help us to infer the mechanical properties of fractures and their immediate surroundings from the breakout observation.

The results of this study provide a better understanding of stress-induced borehole elongations in fractured rocks. The impact of the fracture network on breakout heterogeneities is very pronounced in crystalline rock, which is mechanically isotropic. This is why we could attribute the perturbation of breakouts to the occurrence of fractures and accompanying alteration of mechanical properties only. Numerical modeling taking into account the elastic property changes as a result of fracturing and fracture filling is required to better quantify the breakout orientation heterogeneity that typically observed in many wells.

6. ACKNOWLEDGEMENTS

The authors are grateful to the DIKTI and DAAD for the financial support of the research, to the BRGM for providing the Soultz natural fractures data, and to the GEIE EMC for providing the geophysical log data from the Soultz wells.

REFERENCES

Airy, G. B., On the strains in the interior of beams, *Proceedings of the Royal Society of London*, **12**, (1862), 304-306.

Alm, O., L.-L. Jaktlund, and K. Shaoquan, The influence of microcrack density on the elastic and fracture mechanical properties of Stripa granite, *Physics of the Earth and Planetary Interiors*, **40**, (1985), 161-179.

Barton, C. A., and M. D. Zoback, Stress perturbations associated with active faults penetrated by boreholes: Possible evidence for near-complete stress drop and a new technique for stress magnitude measurement, *Journal of Geophysical Research*, **99**, (1994), 9373-9390.

Bell, J. S., and D. I. Gough, Northeast-southwest compressive stress in Alberta: evidence from oil wells, *Earth and planetary science letters*, **45**, (1979), 475-482.

Chang, C., and B. Haimson, Effect of fluid pressure on rock compressive failure in a nearly impermeable crystalline rock: Implication on mechanism of borehole breakouts, *Engineering Geology*, **89**, (2006), 230-242.

Cornet, F. H., T. Berard, and S. Bourouis, How close to failure is a granite rock mass at a 5 km depth?, *International Journal of Rock Mechanics and Mining Sciences*, **44**, (2007), 47-66.

Ewy, R. T., Yield and closure of directional and horizontal wells, *International Journal of Rock Mechanics and Mining Sciences & Geomechanics*, **30(7)**, (1993), 1061-1067.

Faulkner, D. R., T. M. Mitchell, D. Healy, and M. J. Heap, Slip on 'weak' faults by the rotation of regional stress in the fracture damage zone, *Nature*, **444**, (2006), 922-925.

Heap, M. J., and D. R. Faulkner, Quantifying the evolution of static elastic properties as crystalline rock approaches failure, *International Journal of Rock Mechanics and Mining Sciences*, **45**, (2008), 564-573.

Heap, M. J., D. R. Faulkner, P. G. Meredith, and S. Vinciguerra, Elastic moduli evolution and accompanying stress changes with increasing crack damage: implication for stress change around fault zones and volcanoes during deformation, *Geophysical Journal International*, **183**, (2010), 225-236.

Heidbach, O., J. Reinecker, M. Tingay, B. Müller, B. Sperner, K. Fuchs, and F. Wenzel, Plate boundary forces are not enough: Second- and third-order stress patterns highlighted in the World Stress Map database, *Tectonics*, **26(6)**, (2007), TC6014.

Hurd, O., and M. D. Zoback, Intraplate earthquakes, regional stress and fault mechanics in the Central and Eastern U.S. and Southeastern Canada, *Tectonophysics*, **581**, (2012), 182-192.

Kemeny, J., and N. G. W. Cook, Effective moduli, non-linear deformation and strength of a cracked elastic solid, *International Journal of Rock Mechanics and Mining Sciences*, **23**, (1986), 107-118.

Moos, D., P. Peska, T. Finkbeiner, and M. D. Zoback, Comprehensive wellbore stability analysis utilizing quantitative risk assesment, *Journal of Petroleum Science and Engineering*, **38**, (2003) 97-109.

Müller, B., V. Wehrle, H. Zeyen, and K. Fuchs, Short-scale variations of tectonics regimes in the western European stress province north of the Alps and Pyrenees, *Tectonophysics*, **275**, (1997), 199-219.

Paillet, F. L., and K. Kim, Character and Distribution of Borehole Breakouts and Their Relationship to in Situ Stresses in Deep Columbia River Basalts, *Journal of Geophysical Research*, **92**, (1987), 6223-6234.

Sahara, D., M. Schoeball, T. Kohl, and B. I. R. Mueller, Impact of fracture networks on borehole breakout heterogeneities in crystalline rock, *International Journal of Rock Mechanics and Mining Science*, (submitted)

Scholz, C. H., The mechanics of earthquake and faulting - 2nd edition, 466 pp., *Cambridge University press*, Cambridge, (2002)

Shamir, G., Crustal stress orientation profile to a depth of 3.5km near the San Andreas fault at Cajon Pass, California, 98 pp, Stanford University, Stanford, (1990).

Shamir, G., and M. D. Zoback, Stress orientation profile to 3.5 km depth near the San Andreas Fault at Cajon Pass, California, *Journal of Geophysical Research*, **97(B4)**, (1992), 5059-5080.

Sibson, R. H., Fault rocks and fault mechanisms, *Journal of the Geological Society*, **133**, (1977)191-213.

Sikaneta, S., and K. F. Evans, Stress heterogeneity and natural fractures in the Basel EGS granite reservoir inferred from an acoustic televiewer inferred from an acoustic televiewer log of the Basel-1 Well, paper presented *at Thirty-seventh workshop on geothermal reservoir engineering, Stanford*, (2012)

Timoshenko, S. P., and J. N. Goodier (Eds.), Theory of Elasticity, 3rd edition, Wiley, Newyork, (1970)

Valley, B. C., The relation between natural fracturing and stress heterogeneities in deep-seated crystalline rocks at Soultz-sous-Forets (France), 241 pp, Swiss Federal Institute of Technology Zurich, Zurich., (2007)

Valley, B. C., and K. F. Evans, Stress state at Soultz-sous-Foretz to 5 km depth from wellbore failure and hydraulic observations, paper presented at *Thirty-Second Workshop on Geothermal Reservoir Engineering*, Stanford, US, (2007).

Vermilye, J. M., and C. H. Scholz, The process zone: A microstructural view of fault growth, *Journal of Geophysical Research*, **103**, (1998), 12223-12237.
Zang, A., K. Wolter, and H. Berckhemer, Strain recovery, microcracks and elastic anisotropy of drill cores from KTB deep well, *Scientific drilling: geophysics, geochemistry and technology*, **1**, (1989), 115-126.
Ziegler, P. A., Cenozoic rift system of western and central Europe: an overview, *Geologie en Mijnbouw*, **73**, (1994), 99-127.
Zoback, M. D., Reservoir Geomechanics, Cambridge University Press, New York, (2007)
Zoback, M. D., D. Moos, L. Mastin, and R. N. Anderson, Wellbore breakouts and in situ stress, *Journal of Geophysical Research*, **90**, (1985), 5523-5530